Activation of Gas-Phase Uranyl: From an Oxo to a Nitrido Complex

ARTICLE *in* THE JOURNAL OF PHYSICAL CHEMISTRY A · JANUARY 2014

Impact Factor: 2.69 · DOI: 10.1021/jp4113798 · Source: PubMed

5 AUTHORS, INCLUDING:

Valérie Vallet

French National Centre for Scientific Research

93 PUBLICATIONS **1,856** CITATIONS

SEE PROFILE

THE JOURNAL OF PHYSICAL CHEMISTRY A

Article

pubs.acs.org/JPCA

Activation of Gas-Phase Uranyl: From an Oxo to a Nitrido Complex

Yu Gong,[†] Valérie Vallet,[‡] Maria del Carmen Michelini,[§] Daniel Rios,[†] and John K. Gibson[†,*]

[†]Chemical Sciences Division, Lawrence Berkeley National Laboratory, Berkeley, California 94720, United States

[‡]Université Lille 1 (Sciences et Technologies), Laboratoire PhLAM, CNRS UMR 8523, Bât P5, F-59655, Villeneuve d'Ascq Cedex, France

[§]Dipartimento di Chimica, Università della Calabria, 87030 Arcavacata di Rende, Italy

Supporting Information

ABSTRACT: The uranyl moiety, UO_2^{2+}, is ubiquitous in the chemistry of uranium, the most prevalent actinide. Replacing the strong uranium−oxygen bonds in uranyl with other ligands is very challenging, having met with only limited success. We report here uranyl oxo bond activation in the gas phase to form a terminal nitrido complex, a previously elusive transformation. Collision induced dissociation of gas-phase $UO_2(NCO)Cl_2^-$ in an ion trap produced the nitrido oxo complex, $NUOCl_2^-$, and CO_2. $NUOCl_2^-$ was computed by DFT to have C_s symmetry and a singlet ground state. The computed bond length and order indicate a triple U−N bond. Endothermic activation of $UO_2(NCO)Cl_2^-$ to produce $NUOCl_2^-$ and neutral CO_2 was computed to be thermodynamically more favorable than NCO ligand loss. Complete reaction pathways for the CO_2 elimination process were computed at the DFT level.

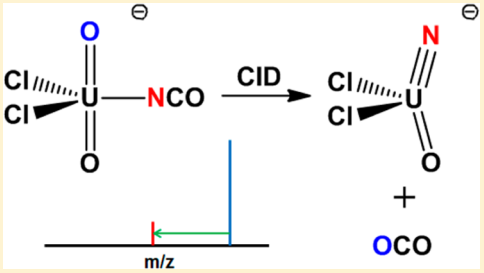

INTRODUCTION

Uranyl, UO_2^{2+}, the most common uranium moiety, is largely inert due to remarkably strong O−U−O bonds.[1,2] As a result, chemistry involving uranyl oxo bond activation has been much less investigated compared with that of transition metal analogues.[3,4] Despite the challenges in the activation and functionalization of uranyl oxo bond, progress has been made in recent years,[5−7] with several examples of uranyl oxo-activation reported.[5] Coordination of Lewis acids such as alkali metals and $B(C_6F_5)_3$ to the yl oxygen of uranyl can substantially reduce the UO bond strength.[8,9] Another synthetic approach to uranyl oxo bond activation is reductive silylation.[10−12] There are several examples of uranium nitride complexes.[13−16] However, to the best of our knowledge there is no report of the direct conversion of a uranyl oxo bond to a nitrido bond.

Gas-phase studies provide detailed information to understand the bond activation process, that can illuminate more complex phenomena which occur in condensed phase, as has been demonstrated by the large body of work on C−H bond activation.[17−19] For uranyl, we recently reported the yl oxygen exchange with UO_2^+ by using mass spectrometry and density functional theory (DFT) calculations.[20] The appearance of $U^{16}O^{18}O^+$ from the thermal reaction of $U^{16}O_2^+$ and $H_2{}^{18}O$ indicated that uranyl activation occurs in the gas phase, and that it might be possible to disrupt the oxo bonds and replace the O atom with a heteroatom, such as N, using appropriate ligated uranyl complexes. Herein, a new type of reaction to induce uranyl activation is reported, which involves transformation of gas-phase $UO_2(NCO)Cl_2^-$ to $NUOCl_2^-$. Collision induced dissociation (CID) of the $UO_2(NCO)Cl_2^-$ complex prepared via electrospray ionization (ESI) produced CO_2 and $NUOCl_2^-$, in which one of the remarkably strong oxo bonds was eliminated and replaced by a nitride bond. Terminal uranium nitride molecules have been identified in the gas phase and solid matrices.[21−25] The first isolated uranium nitride compounds were reported very recently, where the triple U≡N bond was found to be comparable to those of transition metals.[26,27] However, all observed uranium nitride molecules and compounds were made from laser-ablated atoms, uranium metal, or low valent uranium compounds; direct formation of a nitrido from uranyl has not been reported before.

EXPERIMENTAL DETAILS

The experiments reported here were performed using an Agilent 6340 quadrupole ion trap mass spectrometer (QIT/MS) with an orthogonal electrospray ionization (ESI) source inside a radiological contaminant glovebox, as described in detail elsewhere.[28] The $UO_2(NCO)Cl_2^-$ anion complex was produced by ESI of methanol solutions containing $U^{VI}O_2Cl_2$ and NaNCO ($U^{VI}O_2Cl_2$:NaNCO = 1:5, 200 μM $U^{VI}O_2Cl_2$). The pH of the ~20 mM $U^{VI}O_2Cl_2$ stock solution is about 2; the ESI solutions were prepared by dilution in methanol by a factor of ~100×. The MS^n CID capabilities of the QIT/MS allow isolation of ions with a particular mass-to-charge ratio, m/z, and subsequent insertion of an ion−molecule reaction time without applying ion excitation. In high resolution mode, the instrument has a detection range of 20−2200 m/z with a mass width (fwhm) of ~0.3 m/z. Mass spectra were recorded in the

Received: November 19, 2013
Revised: December 18, 2013
Published: December 19, 2013

negative ion accumulation and detection mode. Spectra were taken with the following instrumental parameters: solution flow rate, 60 μL h^{-1}; nebulizer gas pressure, 15 psi; capillary voltage and current, 4000 V; end plate voltage offset and current, −500 V; dry gas flow rate, 5 L min^{-1}; dry gas temperature, 325 °C; capillary exit, −137.5 V; skimmer, −33.4 V; octopole 1 and 2 DC, −10.4 and 0 V; octopole RF amplitude, 300.0 Vpp; lens 1 and 2, 4.3, and 74.5 V; trap drive, 50.8 V. High-purity nitrogen gas for nebulization and drying in the ion transfer capillary was supplied from the boil-off of a liquid nitrogen Dewar. As has been discussed elsewhere,[29−31] the background water and O_2 pressure in the ion trap is estimated to be on the order of 10^{-6} Torr. The helium buffer gas pressure in the trap is constant at ~10^{-4} Torr.

COMPUTATIONAL METHODOLOGY

Small-core relativistic effective core potentials of the Stuttgart-Cologne group, so-called SDD, were employed for all actinide elements[32] along with the segmented basis set,[33] corresponding to the (14s13p10d8f6g)/[10s9p5d4f3g] contraction. Triple-zeta with diffuse function basis sets were used for all light elements ((6-311+G(2d)).[34] The structures of the various isomers, reaction intermediates, and transition states were optimized using two different density functionals (B3LYP[35,36] and TPSSH[37]). A comparison of the bond distances of optimized minima and transition states obtained with the two different density functionals differ by less than 0.03 Å. Geometry optimizations and frequency calculations were performed using the Gaussian09 (revision C01) quantum chemistry package.[38] All transition states were confirmed using the intrinsic reaction coordinates approach (IRC).[39,40] Single-point CCSD(T) calculations were then performed at the optimized geometries of reactants and products using the parallel resolution of the identity approximation,[41] with the appropriate atomic auxiliary basis functions.[42,43] QTAIM analysis[44] was performed on reactants and products in order to analyze the uranium−ligand chemical bond. Appropriate wave function extended files (wfx) were obtained with Gaussian09 and analyzed using AIMAll package.[45]

RESULTS AND DISCUSSION

ESI of UO_2Cl_2 and NaNCO mixtures in methanol resulted in the formation of gas-phase $UO_2(NCO)_xCl_{3-x}^-$ (x = 0−3) complexes. The relative abundances of the different compositions, i.e., values of x, depend on the UO_2Cl_2/NaNCO ratio as well as the pH of UO_2Cl_2 stock solution; the pH dependence was explored using different stock solutions from that noted above. Experimental conditions were optimized such that the $UO_2(NCO)Cl_2^-$ complex was the dominant NCO containing species in the mass spectrum. The choice of this particular precursor with two chloride ligands enables definitive assignment of the uranyl activation product. Precursor complexes comprising more than one NCO ligand, which are easier to produce, introduce ambiguities due to alternative potential ligand isomer structures. The $UO_2(NCO)Cl_2^-$ (m/z 382) complex was mass selected from the parent mass spectrum and subjected to CID, which resulted primarily in a single fragmentation product at m/z 338 as shown in Figure 1. The loss of m/z 44 indicates the loss of CO_2 and formation of $NUOCl_2^-$; the use of the $UO_2(NCO)Cl_2^-$ precursor allows unambiguous assignment of the m/z 44 loss to CO_2 and obviates the necessity for isotopic substitution for confirmation.

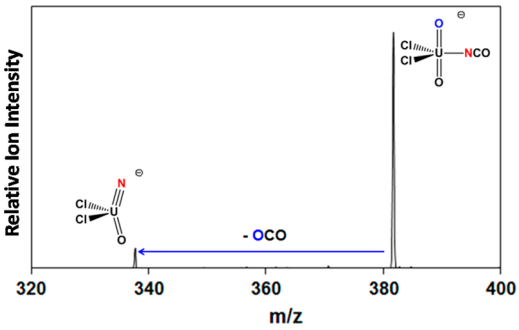

Figure 1. CID mass spectrum of $UO_2(NCO)Cl_2^-$. The loss of m/z 44 provides definitive evidence for elimination of CO_2 from the complex.

Because the U−Cl bond is much stronger than N−Cl and O−Cl bonds,[46,47] it is confidently concluded that both chlorine atoms remain bound to uranium in $NUOCl_2^-$. Although a uranium−nitric oxide complex, $(NO)UCl_2^-$ or $(ON)UCl_2^+$, may be feasible isomer of $NUOCl_2^-$, it is thermodynamically unfavorable to form a N−O bond while disrupting the strong U−N and U−O bonds.[46] This interpretation is supported by reactions of laser-ablated uranium atoms and NO in solid neon, where linear NUO^+, rather than $U(NO)^+$ or $U(ON)^+$, was identified.[22] Furthermore, uranium can readily accommodate a coordination number of 4 with each of the N and O and two Cl atoms directly bound to the uranium metal center. As a result, the $NUOCl_2^-$ complex produced during CID is confidently assigned as a nitrido oxo complex. The result that a peak at m/z 370 was not observed upon CID indicates that O_2 addition to $NUOCl_2^-$ did not occur; this suggests that $NUOCl_2^-$ is a U(VI) complex because U(V) complexes characteristically oxidize to U(VI) superoxides by addition of O_2 under the experimental conditions employed here, as has been discussed elsewhere.[47,48]

CID of $UO_2(NCO)_3^-$ also resulted in the loss of CO_2 to give a product ion with composition $UON(NCO)_2^-$. However, the results for $UO_2(NCO)Cl_2^-$ are emphasized here because of potential alternative structures for the product with two isocyanate ligands. It is probable that CO_2 elimination would have similarly been observed for other $UO_2(NCO)X_2^-$ complexes where X is an anion ligand such as F. The phenomenon of CO_2 elimination to produce $NUOX_2^-$ is presumably not limited to X = Cl; the chloride complex was selected to provide a straightforward and unambiguous demonstration of the phenomenon.

Computational studies were performed to obtain insights into the structure of $NUOCl_2^-$, which was found to have C_s symmetry and a closed-shell singlet ground state (GS). The computed U−O and U−N bond lengths are 1.810 and 1.736 Å, respectively, about 0.03 Å longer than those for the extensively studied triatomic NUO^+ with both DFT and high level ab initio calculations.[49−52] The solid state structures of uranium oxo imido complexes have been reported, which revealed similar U−O bond lengths to that of $NUOCl_2^-$ computed here.[53] However, the double U−N bond length of the imido complexes are about 0.1 Å longer than that of $NUOCl_2^-$, suggesting a stronger U−N bond in $NUOCl_2^-$. The AIM topological values at the bond critical points suggest that the U−N bond is stronger and more covalent than the U−O bond; that is, the density ρ_b is larger and the energy density H is more negative for the U−N bond than for the U−O bond (Table 1). This is consistent with the computed Mayer (M) and

dx.doi.org/10.1021/jp4113798 | J. Phys. Chem. A 2014, 118, 325−330

Table 1. Electron Densities (ρ) and Energy Densities (H) at Selected Bond Critical Points, and Mayer Bond Order (M-BO), and Gophinatan-Jug Bond Orders (GJ-BO) for the Ground State and Isomer 1 Structures of $UO_2(NCO)Cl_2^-$, and for the Product $NUOCl_2^-$

	$UO_2(NCO)Cl_2^-$ GS	$UO_2(NCO)Cl_2^-$ Isomer 1	$NUOCl_2^-$ Product
		U−O_{ax}	
ρ	0.307	0.277	0.277
H	−0.273	−0.219	−0.226
M-BO	1.99	2.04	1.94
GJ-BO	2.29	2.37	2.31
		U−O_{eq}	
ρ	-	0.262	-
H	-	−0.195	-
M-BO	-	2.03	-
GJ-BO	-	2.33	-
		U−N_{ax}	
ρ	-	-	0.365
H	-	-	−0.396
M-BO	-		2.94
GJ-BO	-	-	2.99
		U−NCO	
ρ	0.086	0.099	-
H	−0.018	−0.027	-
M-BO	0.61	0.69	-
GJ-BO	0.78	0.87	-
		U−Cl	
ρ	0.068	0.069	0.064
H	−0.016	−0.016	−0.014
M-BO	0.88	0.91	0.79
GJ-BO	0.97	0.99	0.89

Gophinatan-Jug (GJ) bond orders: the computed M and GJ U−N bond orders in $NUOCl_2^-$ are 2.9 and 3.0, respectively, while those of the U−O bond are close to 1.9 and 2.3, respectively (Table 1). There is no significant difference between the computed bond orders of the U−O_{ax} bonds in the $UO_2(NCO)Cl_2^-$ uranyl complex and the U−O_{ax} bond in the $NUOCl_2^-$ nitrido complex (O_{ax} denotes the axial oxygen, commonly referred to as O_{yl} in uranyl). An interesting result of the bonding analysis for Isomer 1 (see Table 1; structure in Figure S1) is that the U−O_{eq} bond (i.e., the uranium bond to the equatorial oxygen atom) is essentially as covalent as the U−O_{ax} bond. The triatomic NUO^+ cation has been observed in the gas phase by mass spectrometry and in cryogenic matrices by infrared spectroscopy.[21,22] Based on calculations at different levels of theory,[49−52] a linear geometry with terminal nitrido and oxo bonds was established. In contrast to bare NUO^+, the computed NUO bond angle in $NUOCl_2^-$ is 28° distorted from linear NUO^+. A more moderate distortion from linearity has been observed for a recently synthesized uranium oxo nitrido complex, where the NUO bond angle is 167.6°.[54] Despite such distortion, the UN and UO bonds are not necessarily substantially disrupted, since the triple U−N and double U−O (formally triple[1]) bond characters are maintained in $NUOCl_2^-$, as evidenced by the slight increase in bond lengths.

Geometry optimizations were performed for different structural isomers of the reactant $UO_2(NCO)Cl_2^-$ complex (Figure S1). Ground-state $UO_2(NCO)Cl_2^-$ was computed to have C_{2v} structure while an isomer 59 kJ.mol^{-1} higher in energy possesses a C_s structure, with the CN subunit distorted from the equatorial plane. The reaction to form $NUOCl_2^-$ from $UO_2(NCO)Cl_2^-$ (reaction 1) occurs under energetic CID conditions. On the basis of our CCSD(T) calculations, this conversion is endothermic by 267 kJ.mol^{-1} (256 kJ.mol^{-1} at DFT-B3LYP level). This high reaction energy is attributed to the very strong UO bond in the precursor,[2] which renders uranyl activation much more energetically demanding than for transition metal analogues.[3,4] CID reaction 1 is thermodynamically facilitated by the formation of the stable CO_2 molecule; the formation of two molecules from one furthermore results in a favorably reaction entropy.

$$UO_2(NCO)Cl_2^- \rightarrow NUOCl_2^- + CO_2 \quad (1)$$

Alternative reactions to the observed CO_2 loss were also considered (Table 2). The optimized geometries of all the alternative reaction products are included as Supporting Information (Figure S2). It was found that CO_2 loss is the thermodynamically most favorable process. Ligand-loss CID processes, which are observed in CID of some ligated uranyl complexes,[55] were computed to be higher in energy than reaction 1 by about 50−100 kJ.mol^{-1}, in accord with their non-observation here. The loss of Cl^-, computed as the most favorable ligand-loss channel, is more endothermic than CO_2 loss by 56 kJ.mol^{-1}.

Table 2. Computed Reaction Energies for Ligand Loss Reactions[a]

	ΔE/kJ.mol^{-1}
$UO_2(NCO)Cl_2^-$ (1) → $NUOCl_2^-$ (1) + CO_2 (1)	256
$UO_2(NCO)Cl_2^-$ (1) → $UO_2(NCO)Cl$ (1) + Cl^- (1)	312
$UO_2(NCO)Cl_2^-$ (1) → UO_2Cl_2 (1) + NCO^- (1)	327
$UO_2(NCO)Cl_2^-$ (1) → $UO_2Cl_2^-$ (2) + NCO (2)	347
$UO_2(NCO)Cl_2^-$ (1) → $UO_2(NCO)Cl^-$ (2) + Cl (2)	356

[a]B3LYP/SDD level, ZPE correction included; spin multiplicities given in parentheses; computed product structures shown in Figure S2.

Complete reaction pathways for CO_2 elimination were computed at the DFT level (Figure 2). The optimized geometries of all the species involved in the reaction pathways

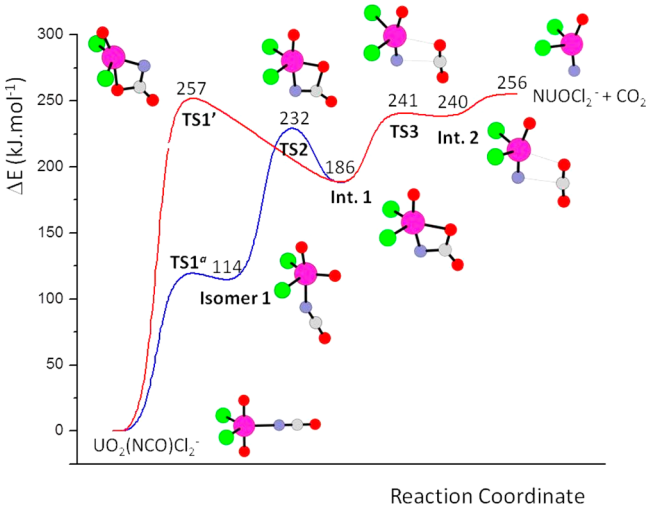

Figure 2. $UO_2(NCO)Cl_2^-$ → $NUOCl_2^-$ + CO_2 potential energy profile computed at the B3LYP/SDD level of theory. See Figure S2 for all geometrical parameters. ([a]For details regarding TS1 see Figure S3.)

dx.doi.org/10.1021/jp4113798 | J. Phys. Chem. A 2014, 118, 325−330

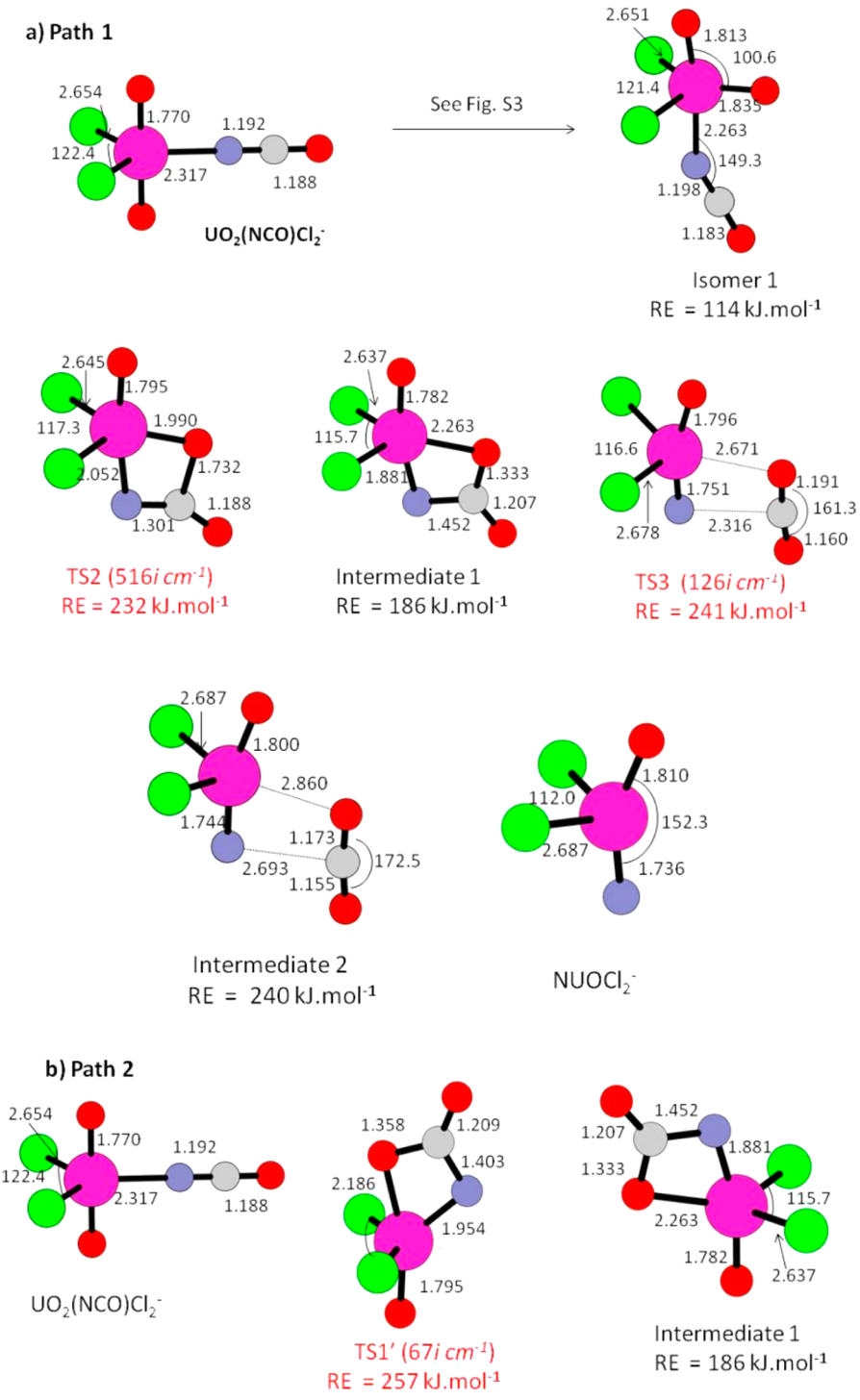

Figure 3. Optimized geometrical parameters of all the minima and transition states involved in the $UO_2(NCO)Cl_2^-$ → $NUOCl_2^-$ + CO_2 reaction pathways (B3LYP/SDD). Bond lengths are in angstroms and angles are in degrees. RE is the relative energy with respect to the $UO_2(NCO)Cl_2^-$ ground state. Transition state imaginary frequencies are given in parentheses. Path 1 and Path 2 coincide from the intermediate 1 to product formation.

are shown in Figure 3. Transition state imaginary frequencies are reported in Figure 3. The lowest-energy reaction pathway involves the initial conversion of the $UO_2(NCO)Cl_2^-$ GS reactant to an isomer containing the NCO group in an axial position (Isomer 1). It was not possible to locate the transition state TS1 connecting these two isomers. However, relaxed scan calculations suggest that this conversion proceeds without significant barriers in excess of the endothermicity of the process such that TS1 could not be identified. In the relaxed scan calculations the OUN angle was used as the scanning parameter, with an incremental step size of 5°. The starting point was the $UO_2(NCO)Cl_2^-$ GS structure with an OUN angle of ca. 90°; the final OUN angle was ca. 180°. The rest of the variables were fully optimized at each point of the scan. The obtained results, summarized in Figure S3, reveal that the barrier between the GS and Isomer 1 of $UO_2(NCO)Cl_2^-$ is

dx.doi.org/10.1021/jp4113798 | J. Phys. Chem. A 2014, 118, 325−330

minuscule, consistent with our inability to locate the transition state between the two. Isomer 1 converts to Intermediate 1 via transition state TS2 by interaction of the C-atom in the axial NCO ligand with the equatorial O-atom. The vibrational mode associated with the TS2 imaginary frequency (516*i* cm^{-1}) corresponds to the expected motion of the atoms associated with the transformation. The ultimate CO_2 elimination proceeds from Intermediate 1 in a straightforward manner (TS2 and Intermediate 1 have a similar arrangement of atoms, but differ in bond distances; see Figure 3). The key aspects of this mechanism are similar to the reverse of that proposed for activation of CO_2 by high-valent uranium complexes.[56] In an alternative pathway (Figure 2), the initial complex converts directly to Intermediate 1 via a transition state (TS1′) that is slightly higher in energy than TS2. In TS1′ the C-atom in the NCO ligand interacts with the axial O-atom; a geometrical rearrangement results in Intermediate 1, which is common to both pathways. The vibrational mode associated with the TS1′ imaginary frequency (67*i* cm^{-1}) involves a rocking movement (in the plane containing the UO_2−NCO atoms) of the U−O_{ax} bond not involved in the interaction with NCO. Under CID conditions, both energetically comparable pathways are feasible, with transition state energies lying at least 50 kJ.mol^{-1} below the endothermicity of all ligand loss processes, which are presumably nearly barrierless.

CONCLUSIONS

A new type of uranyl oxo bond activation was observed in the gas phase. CID of $UO_2(NCO)Cl_2^-$ resulted in the formation of $NUOCl_2^-$, concomitant with elimination of CO_2, where one of the uranium oxo bonds is replaced by a terminal uranium nitrido bond. DFT calculations revealed that $NUOCl_2^-$ possesses C_s symmetry and closed shell singlet ground state. A triple U−N bond was identified on the basis of the short U−N distance and the computed Mayer and Gophinatan-Jug bond orders. Although the activation process is endothermic, the energy provided by CID is sufficient to enable this reaction in the gas phase. Alternative ligand-loss processes were computed to be higher in energy. Reaction pathways were computed at the DFT-B3LYP level for the observed uranyl activation process that results in transformation of a OUO complex to a NUO complex.

ASSOCIATED CONTENT

Supporting Information

Optimized geometries of different $UO_2(NCO)Cl_2^-$ isomers and of alternative $UO_2(NCO)Cl_2^-$ dissociation products. Summary of relaxed scan calculations for the conversion of two different $UO_2(NCO)Cl_2^-$ structural isomers. This material is available free of charge via the Internet at http://pubs.acs.org.

AUTHOR INFORMATION

Corresponding Author

*E-mail: jkgibson@lbl.gov.

Notes

The authors declare no competing financial interest.

ACKNOWLEDGMENTS

This work was supported by the U.S. Department of Energy, Office of Basic Energy Sciences, Heavy Element Chemistry, at LBNL under Contract No. DE-AC02-05CH11231 [Y.G., D.R., J.K.G.], by CNRS and French Ministère de l'Enseignement Supérieur et de la Recherche [V.V.], and by the Università della Calabria [M.C.M.]. This research used resources of the National Energy Research Scientific Computing Center (NERSC), which is supported by the Office of Science of the U.S. Department of Energy under Contract No. DE-AC02-05CH11231, as well as the use of HPC resources from GENCI-CCRT (Grants 2012-081859 and 2013-081859).

REFERENCES

(1) Denning, R. G. Electronic Structure and Bonding in Actinyl Ions and Their Analogs. *J. Phys. Chem. A* **2007**, *111*, 4125−4143.
(2) Marçalo, J.; Gibson, J. K. Gas-Phase Energetics of Actinide Oxides: An Assessment of Neutral and Cationic Monoxides and Dioxides from Thorium to Curium. *J. Phys. Chem. A* **2009**, *113*, 12599−12606.
(3) Kühn, F. E.; Santos, A. M.; Abrantes, M. Mononuclear Organomolybdenum(VI) Dioxo Complexes: Synthesis, Reactivity, and Catalytic Applications. *Chem. Rev.* **2006**, *106*, 2455−2475.
(4) Mayer, J. M. Hydrogen Atom Abstraction by Metal-Oxo Complexes: Understanding the Analogy with Organic Radical Reactions. *Acc. Chem. Res.* **1998**, *31*, 441−450.
(5) Fortier, S.; Hayton, T. W. Oxo Ligand Functionalization in the Uranyl Ion (UO_2^{2+}). *Coord. Chem. Rev.* **2010**, *254*, 197−214.
(6) Jones, M. B.; Gaunt, A. J. Recent Developments in Synthesis and Structural Chemistry of Nonaqueous Actinide Complexes. *Chem. Rev.* **2013**, *113*, 1137−1198.
(7) Baker, R. J. New Reactivity of the Uranyl(VI) Ion. *Chem.—Eur. J.* **2012**, *18*, 16258−16271.
(8) Arnold, P. L.; Pecharman, A. F.; Hollis, E.; Yahia, A.; Maron, L.; Parsons, S.; Love, J. B. Uranyl Oxo Activation and Functionalization by Metal Cation Coordination. *Nat. Chem.* **2010**, *2*, 1056−1061.
(9) Sarsfield, M. J.; Helliwell, M. Extending the Chemistry of the Uranyl Ion: Lewis Acid Coordination to a U═O Oxygen. *J. Am. Chem. Soc.* **2004**, *126*, 1036−1037.
(10) Schnaars, D. D.; Wu, G.; Hayton, T. W. Silylation of the Uranyl Ion Using $B(C_6F_5)_3$-Activated Et_3SiH. *Inorg. Chem.* **2011**, *50*, 9642−9649.
(11) Arnold, P. L.; Patel, D.; Wilson, C.; Love, J. B. Reduction and Selective Oxo Group Silylation of the Uranyl Dication. *Nature* **2008**, *451*, 315−317.
(12) Berthet, J. C.; Siffredi, G.; Thuery, P.; Ephritikhine, M. Controlled Chemical Reduction of Uranyl Salts into $UX_4(MeCN)_4$ (X = Cl, Br, I) with Me_3SiX Reagents. *Eur. J. Inorg. Chem.* **2007**, 4017−4020.
(13) Duval, P. B.; Burns, C. J.; Buschmann, W. E.; Clark, D. L.; Morris, D. E.; Scott, B. L. Reaction of the Uranyl(VI) ion (UO_2^{2+}) with a Triamidoamine Ligand: Preparation and Structural Characterization of a Mixed-Valent Uranium(V/VI) Oxo-Imido Dimer. *Inorg. Chem.* **2001**, *40*, 5491−5496.
(14) Nocton, G.; Pécaut, J.; Mazzanti, M. A Nitrido-Centered Uranium Azido Cluster Obtained from a Uranium Azide. *Angew. Chem., Int. Ed.* **2008**, *47*, 3040−3042.
(15) Fox, A. R.; Cummins, C. C. Uranium-Nitrogen Multiple Bonding: The Case of a Four-Coordinate Uranium(VI) Nitridoborate Complex. *J. Am. Chem. Soc.* **2009**, *131*, 5716−5717.
(16) Hayton, T. W. Recent Developments in Actinide-Ligand Multiple Bonding. *Chem. Commun.* **2013**, *49*, 2956−2973.
(17) Roithová, J.; Schröder, D. Selective Activation of Alkanes by Gas-Phase Metal Ions. *Chem. Rev.* **2010**, *110*, 1170−1211.
(18) Schröder, D.; Schwarz, H. Gas-Phase Activation of Methane by Ligated Transition-Metal Cations. *Proc. Natl. Acad. Sci. U.S.A.* **2008**, *105*, 18114−18119.
(19) Schwarz, H. Chemistry with Methane: Concepts Rather than Recipes. *Angew. Chem., Int. Ed.* **2011**, *50*, 10096−10115.
(20) Rios, D.; Michelini, M. C.; Lucena, A. F.; Marçalo, J.; Gibson, J. K. On the Origins of Faster Oxo Exchange for Uranyl(V) versus Plutonyl(V). *J. Am. Chem. Soc.* **2012**, *134*, 15488−15496.

(21) Heinemann, C.; Schwarz, H. NUO^+, a New Species Isoelectronic to the Uranyl Dication UO_2^{2+}. *Chem.—Eur. J.* **1995**, *1*, 7−11.
(22) Zhou, M. F.; Andrews, L. Infrared Spectra and Pseudopotential Calculations for NUO^+, NUO, and NThO in Solid Neon. *J. Chem. Phys.* **1999**, *111*, 11044−11049.
(23) Hunt, R. D.; Yustein, J. T.; Andrews, L. Matrix Infrared-Spectra of NUN Formed by the Insertion of Uranium Atoms into Molecular Nitrogen. *J. Chem. Phys.* **1993**, *98*, 6070−6074.
(24) Wang, X. F.; Andrews, L.; Vlaisavljevich, B.; Gagliardi, L. Combined Triple and Double Bonds to Uranium: The N≡U═N-H Uranimine Nitride Molecule Prepared in Solid Argon. *Inorg. Chem.* **2011**, *50*, 3826−3831.
(25) Andrews, L.; Wang, X. F.; Lindh, R.; Roos, B. O.; Marsden, C. J. Simple $N{\equiv}UF_3$ and $P{\equiv}UF_3$ Molecules with Triple Bonds to Uranium. *Angew. Chem., Int. Ed.* **2008**, *47*, 5366−5370.
(26) King, D. M.; Tuna, F.; McInnes, E. J. L.; McMaster, J.; Lewis, W.; Blake, A. J.; Liddle, S. T. Isolation and Characterization of a Uranium(VI)-Nitride Triple Bond. *Nat. Chem.* **2013**, *5*, 482−488.
(27) King, D. M.; Tuna, F.; McInnes, E. J. L.; McMaster, J.; Lewis, W.; Blake, A. J.; Liddle, S. T. Synthesis and Structure of a Terminal Uranium Nitride Complex. *Science* **2012**, *337*, 717−720.
(28) Rios, D.; Rutkowski, P. X.; Shuh, D. K.; Bray, T. H.; Gibson, J. K.; Van Stipdonk, M. J. Electron Transfer Dissociation of Dipositive Uranyl and Plutonyl Coordination Complexes. *J. Mass Spectrom.* **2011**, *46*, 1247−1254.
(29) Rutkowski, P. X.; Michelini, M. C.; Gibson, J. K. Proton Transfer in Th(IV) Hydrate Clusters: A Link to Hydrolysis of $Th(OH)_2^{2+}$ to $Th(OH)_3^+$ in Aqueous Solution. *J. Phys. Chem. A* **2013**, *117*, 451−459.
(30) Rutkowski, P. X.; Michelini, M. C.; Bray, T. H.; Russo, N.; Marçalo, J.; Gibson, J. K. Hydration of Gas-Phase Ytterbium Ion Complexes Studied by Experiment and Theory. *Theor. Chem. Acc.* **2011**, *129*, 575−592.
(31) Rios, D.; Michelini, M. C.; Lucena, A. F.; Marçalo, J.; Bray, T. H.; Gibson, J. K. Gas-Phase Uranyl, Neptunyl, and Plutonyl: Hydration and Oxidation Studied by Experiment and Theory. *Inorg. Chem.* **2012**, *51*, 6603−6614.
(32) Küchle, W.; Dolg, M.; Stoll, H.; Preuss, H. Energy-Adjusted Pseudopotentials for the Actinides - Parameter Sets and Test Calculations for Thorium and Thorium Monoxide. *J. Chem. Phys.* **1994**, *100*, 7535−7542.
(33) Cao, X. Y.; Dolg, M.; Stoll, H. Valence Basis Sets for Relativistic Energy-Consistent Small-Core Actinide Pseudopotentials. *J. Chem. Phys.* **2003**, *118*, 487−496.
(34) Krishnan, R.; Binkley, J. S.; Seeger, R.; Pople, J. A. Self-Consistent Molecular-Orbital Methods 0.20. Basis Set for Correlated Wave-Functions. *J. Chem. Phys.* **1980**, *72*, 650−654.
(35) Lee, C. T.; Yang, W. T.; Parr, R. G. Development of the Colle-Salvetti Correlation-Energy Formula into a Functional of the Electron-Density. *Phys. Rev. B* **1988**, *37*, 785−789.
(36) Becke, A. D. Density-Functional Thermochemistry. III. The Role of Exact Exchange. *J. Chem. Phys.* **1993**, *98*, 5648−5652.
(37) Tao, J. M.; Perdew, J. P.; Staroverov, V. N.; Scuseria, G. E. Climbing the Density Functional Ladder: Nonempirical Meta-Generalized Gradient Approximation Designed for Molecules and Solids. *Phys. Rev. Lett.* **2003**, *91*, 146401−1 - 146401−4.
(38) Frisch, M. J.; et al. *Gaussian 2009*, revision B01. See Supporting Information for full citation.
(39) Fukui, K. The path of chemical-reactions - The IRC approach. *Acc. Chem. Res.* **1981**, *14*, 363−368.
(40) Hratchian, H. P.; Schlegel, H. B. In *Theory and Applications of Computational Chemistry: The First 40 Years*; Dykstra, C. E., Frenking, G., Kim, K. S., Scuseria, G. E., Eds.; Elsevier: Amsterdam, 2005; pp 195−249.
(41) Hattig, C.; Hellweg, A.; Kohn, A. Distributed Memory Parallel Implementation of Energies and Gradients for Second-Order Møller-Plesset Perturbation Theory with the Resolution-of-the-Identity Approximation. *Phys. Chem. Chem. Phys.* **2006**, *8*, 1159−1169.
(42) Weigend, F.; Kohn, A.; Hattig, C. Efficient Use of the Correlation Consistent Basis Sets in Resolution of the Identity MP2 Calculations. *J. Chem. Phys.* **2002**, *116*, 3175−3183.
(43) Hattig, C. Optimization of Auxiliary Basis Sets for RI-MP2 and RI-CC2 Calculations: Core-Valence and Quintuple-Zeta Basis Sets for H to Ar and QZVPP Basis Sets for Li to Kr. *Phys. Chem. Chem. Phys.* **2005**, *7*, 59−66.
(44) Bader, R. F. W. *Atoms in Molecules: A Quantum Theory*; Oxford University Press: Oxford, 1990.
(45) Keith, T. A. *AIMAll. 12.06.21*; TK Gristmill Software; Overland Park, KS, USA, 2013.
(46) Lide, D. R. *Handbook of Physics and Chemistry*, 90th ed.; CRC Press: Boca Raton, FL, 2009.
(47) Rios, D.; Michelini, M. C.; Lucena, A. F.; Marçalo, J.; Bray, T. H.; Gibson, J. K. Gas-Phase Uranyl, Neptunyl, and Plutonyl: Hydration and Oxidation Studied by Experiment and Theory. *Inorg. Chem.* **2012**, *51*, 6603−6614.
(48) Gong, Y.; Gibson, J. K. Formation and Characterization of the Uranyl-SO_2 Complex, $UO_2(CH_3SO_2)(SO_2)^-$. *J. Phys. Chem. A* **2013**, *117*, 783−787.
(49) Pyykkö, P.; Li, J.; Runeberg, N. Quasi-Relativistic Pseudopotential Study of Species Isoelectronic to Uranyl and the Equatorial Coordination of Uranyl. *J. Phys. Chem.* **1994**, *98*, 4809−4813.
(50) Wei, F.; Wu, G. S.; Schwarz, W. H. E.; Li, J. Geometries, Electronic Structures, And Excited States of UN_2, NUO^+, and UO_2^{2+}: a Combined CCSD(T), RAS/CASPT2 and TDDFT Study. *Theor. Chem. Acc.* **2011**, *129*, 467−481.
(51) Tecmer, P.; Gomes, A. S. P.; Ekstrom, U.; Visscher, L. Electronic Spectroscopy of UO_2^{2+}, NUO^+ and NUN: an Evaluation of Time-Dependent Density Functional Theory for Actinides. *Phys. Chem. Chem. Phys.* **2011**, *13*, 6249−6259.
(52) Gagliardi, L.; Roos, B. O. Uranium Triatomic Compounds XUY (X,Y = C,N,O): a Combined Multiconfigurational Second-Order Perturbation and Density Functional Study. *Chem. Phys. Lett.* **2000**, *331*, 229−234.
(53) Hayton, T. W.; Boncella, J. M.; Scott, B. L.; Batista, E. R. Exchange of an Imido Ligand in Bis(Imido) Complexes of Uranium. *J. Am. Chem. Soc.* **2006**, *128*, 12622−12623.
(54) Fortier, S.; Wu, G.; Hayton, T. W. Synthesis of a Nitrido-Substituted Analogue of the Uranyl Ion, $[N{=}U{=}O]^+$. *J. Am. Chem. Soc.* **2010**, *132*, 6888−6889.
(55) Groenewold, G. S.; de Jong, W. A.; Oomens, J.; Van Stipdonk, M. J. Variable Denticity in Carboxylate Binding to the Uranyl Coordination Complexes. *J. Am. Soc. Mass Spectrom.* **2010**, *21*, 719−727.
(56) Bart, S. C.; Anthon, C.; Heinemann, F. W.; Bill, E.; Edelstein, N. M.; Meyer, K. Carbon Dioxide Activation with Sterically Pressured Mid- and High-Valent Uranium Complexes. *J. Am. Chem. Soc.* **2008**, *130*, 12536−12546.